Agricultural and Forest Meteorology 259 (2018) 60–74

Contents lists available at ScienceDirect

Agricultural and Forest Meteorology

journal homepage: www.elsevier.com/locate/agrformet

The importance of carbon-nitrogen biogeochemistry on water vapor and carbon fluxes as elucidated by a multiple canopy layer higher order closure land surface model

Kuang-Yu Chang[a,b,c,*], Kyaw Tha Paw U[a], Shu-Hua Chen[a]

[a] Department of Land, Air and Water Resources, University of California, Davis, CA, USA
[b] Earth System Research Center, University of New Hampshire, Durham, NH, USA
[c] Climate and Ecosystem Sciences Division, Lawrence Berkeley National Laboratory, Berkeley, CA, USA

ARTICLE INFO

Keywords:
ACASA
ACASA-CN
ET partitioning
CN biogeochemistry
Land surface model

ABSTRACT

The carbon-nitrogen (CN) biogeochemistry and the prognostic canopy structure scheme used in the Community Land Model version 4.5 (CLM4.5) are integrated into the multiple canopy layer higher order closure Advanced Canopy-Atmosphere-Soil Algorithm (ACASA). The ACASA-CN model inherits the advantages from ACASA and CLM4.5, and it is the first model that represents fully prognostic terrestrial feedbacks with a higher order closure turbulence scheme and vertically resolved canopy structure. The simulations are evaluated in terms of ecological, biogeophysical and biogeochemical aspects at six AmeriFlux eddy covariance sites encompassing a variety of vegetation types and microclimatic conditions across the continental United States. Our model evaluation shows that ACASA-CN reasonably simulates surface layer properties, such as vegetation structure and plant phenology. Our results indicate that the use of a higher order closure turbulence scheme with multiple canopy layer representation is critical to land carbon cycle simulation. Based on our simulations, water vapor exchange between the land surface and the atmosphere is primarily through plant transpiration (78–88%), and canopy evapotranspiration is enhanced with the use of CN biogeochemistry. Our results indicate that the ratio of transpiration to evapotranspiration exhibits a two-stage variation pattern, and the transpiration fraction decreases in dense canopies.

1. Introduction

The physical processes in land surface control the lower boundary conditions for energy, water vapor and momentum in the lower atmosphere; therefore, a reasonable representation for these processes is crucial to regional and global climate simulations (Fatichi et al., 2015). Garratt (1993) reviewed the sensitivity of climate simulations to land surface treatments in different Global Climate Models (GCMs), and found that an appropriate land surface scheme is one major requirement for realistic global climate simulations. Such land surface schemes are necessary to properly represent the effects of soils and vegetation that are critical to terrestrial fluxes and climate simulations (Garratt, 1993; Sellers et al., 1997). In addition to biogeophysical impacts on climate simulations, Cox et al. (2000) demonstrated the importance of biogeochemical feedbacks on twenty-first century climate projections by incorporating a carbon cycle model into a fully coupled GCM. Based on their results, carbon cycle feedbacks could significantly accelerate climate change because the direct effect of CO_2 on photosynthesis rate saturates at higher CO_2 concentrations while a specific soil respiration rate continues to increase with temperature. The atmospheric CO_2 concentration was 250 ppmv higher in their fully coupled carbon simulation than in their uncoupled carbon simulation, resulting in a 1.5 K increase in global mean temperature when carbon cycle feedbacks were activated. Similar results were obtained in Friedlingstein et al. (2006) and Matthews et al. (2007).

However, the strength of carbon cycle feedbacks is regulated by the amount of available nutrients such as nitrogen in ecosystems, and the absence of an explicit treatment of nutrient dynamics in ecosystem simulations increases model uncertainties in the predictions of future atmospheric CO_2 concentration and the associated anthropogenic climate change (Thornton et al., 2009). Studies have shown that the inclusion of fully coupled carbon and nitrogen cycles in land surface schemes can reduce the simulated global terrestrial carbon uptake response to increasing atmospheric CO_2 concentration by 53–78%, relative to a carbon cycle only counterpart model (Thornton et al., 2007; Sokolov et al., 2008). Moreover, Thornton et al. (2007) concluded that

* Corresponding author at: Climate and Ecosystem Sciences Division, Lawrence Berkeley National Laboratory, Berkeley, California, USA.
E-mail address: ckychang@lbl.gov (K.-Y. Chang).

https://doi.org/10.1016/j.agrformet.2018.04.009
Received 20 October 2017; Received in revised form 29 March 2018; Accepted 13 April 2018

the coupling of terrestrial carbon and nitrogen fundamentally impacts climate carbon cycle feedbacks, and the reduction of direct CO_2 fertilization effect cannot be reproduced by simple parameterizations of a carbon only model. Bonan and Levis (2010) quantified the effects of nitrogen dynamics on carbon exchange in the Community Land Model version 4 (CLM4) over the period 1973–2004. Their results suggested that the inclusion of nitrogen cycle would reduce both concentration-carbon feedback and climate-carbon feedback, compared with carbon only biogeochemistry. Several studies have also demonstrated the importance of terrestrial nitrogen feedbacks on the land carbon cycle (Sokolov et al., 2008; Thornton et al., 2009; Zaehle et al., 2010a; 2010b; Friedlingstein et al., 2014).

The effects of carbon-nitrogen (CN) biogeochemistry can also affect vegetation structure that is largely controlled by the trend of the land carbon cycle. Studies have found that changes in vegetation structures can influence the partitioning of latent and sensible heat fluxes and thus impact atmospheric boundary layer development (Foley et al., 2003; Fatichi et al., 2015). For example, stomatal conductance declines when atmospheric CO_2 concentration increases, leading to the reduction of evapotranspiration. This alters surface energy and water vapor fluxes, which in turn affects atmospheric circulation patterns and water cycle over land (Foley et al., 2003; Levis, 2010).

Apart from the impacts by CN biogeochemistry, recent studies have also found that the realism of model description of ecosystem structure and function in surface layer exchange processes is as important as the accuracy of other model physics (Weiss et al., 2012; Weiss et al., 2014; Chang et al., 2018). This is because the type and the density of vegetation control the states of surface, subsurface and atmospheric properties (Douville 2003; Dirmeyer and Zhao 2004), which largely affect ecosystem response and thus regulate local and regional scale climatic conditions (Arora, 2002; Pielke et al., 2011). Weiss et al. (2012) and Chang et al. (2018) have shown that a more realistic surface property description is beneficial to biogeophysical and biogeochemical simulations. However, their analyses did not consider the effects of CN biogeochemistry on the nonlinear interactions between canopy structure and turbulence transports.

This study aims to determine the effects of CN biogeochemistry on terrestrial fluxes, which are important to weather forecasts and climate simulations. In particular, we are interested in effects of CN biogeochemistry on the partitioning of evapotranspiration (ET) into evaporation and transpiration. We use a coupled model that integrates a prognostic canopy structure scheme based on CN biogeochemistry processes into a multiple canopy layer land surface model. More specifically, the CN biogeochemistry submodel in the commonly studied Community Land Model version 4.5 (CLM4.5) is coupled to the Advanced Canopy-Atmosphere-Soil Algorithm (ACASA) that uses carbon only biogeochemistry. ACASA simulates realistic turbulence transports by its third order closure parameterization, and CLM4.5 represents more advanced CN biogeochemistry with simpler turbulence parameterization. The resulting ACASA-CN model simulates fully coupled nonlinear terrestrial interactions with explicit plant traits representation, and it is the first model that uses a higher order closure parameterization and a vertically resolved canopy to represent feedbacks among vegetation structure, plant physiology, nutrient dynamics, and turbulence processes. The model incorporates detailed vertical canopy structural and functional representations, which is beneficial when analyzing the source of fluxes contributed by different parts of the simulated canopy, such as partitioning water vapor flux into evaporation from soil and canopy surfaces and transpiration from plant stomata.

Simulations across various types of ecosystem and microclimatic conditions were compared with remote sensing datasets and in-situ measurements in terms of canopy structure, energy, water vapor, and carbon fluxes. The effects of CN biogeochemistry on terrestrial fluxes simulation were investigated by conducting a series of offline simulations with carbon only biogeochemistry. We hypothesize that stomata controlled transpiration is regulated by the use of biogeochemistry, and the integration of realistic turbulence and advanced biogeochemistry schemes is beneficial to accurate land surface simulation. Continuous eddy covariance measurements were used to evaluate the energy, water vapor and carbon fluxes simulated by ACASA-CN. The amounts of evaporation and transpiration simulated by ACASA-CN using carbon only versus CN biogeochemistry were analyzed to test our hypothesis.

This paper is organized as follows. Section 2 introduces the numerical models and observational datasets used in this study. Simulation results and some relevant discussions are given in section 3. Model sensitivity and the effects of CN biogeochemistry are evaluated in section 4. Concluding remarks are provided in section 5.

2. Methods

2.1. CLM 4.5

The Community Land Model (CLM), which is the land surface component of the Community Earth System Model (CESM), is widely applied in regional and global climate simulations. CLM features a nested subgrid hierarchy, in which each grid cell can be composed of multiple land units, soil columns, and plant functional types (Oleson et al., 2013). This mosaic structure design enables it to efficiently represent complex land surface and subsurface patterns at a global scale. The vegetation canopy is represented by two leaf classes, one sunlit and the other shaded.

Major improvements were made to CLM version 4 (CLM4), including updates to soil hydrology, soil thermodynamics, the snow model, albedo parameters, the land surface types dataset, and the River Transport Model (Lawrence et al., 2011). Moreover, a carbon and nitrogen cycle model that includes prognostic vegetation phenology described in Thornton et al. (2002) and Thornton and Zimmermann (2007) was added to CLM4 to improve the biogeochemical processes in the model.

Several modifications were also applied to CLM version 4.5 (CLM4.5) to reduce the biases found in CLM4 and incorporate the latest scientific understanding of land surface processes (Oleson et al., 2013). The main canopy process modifications are as follows: (1) The use of a revised canopy radiation scheme, co-limitations on the photosynthesis rate, and revisions to the original photosynthetic parameters to fix the gross primary production biases found in CLM4 (Bonan et al., 2011; Bonan et al., 2012). (2) The application of temperature acclimation of photosynthesis, and improved stability of the iterative solution in the photosynthesis and stomatal conductance model (Sun et al., 2012). More detailed descriptions of the CLM4.5 can be found in Oleson et al. (2013).

2.2. ACASA-CN

The Advanced Canopy-Atmosphere-Soil Algorithm (ACASA) is a multiple canopy layer turbulence land surface model based on the diabatic third order closure method developed by Meyers and Paw U (1986; 1987). The multiple canopy layer and third order closure features enable ACASA to simulate realistic turbulent transports of energy, water vapor, momentum and carbon flux within and above vegetation canopies (Meyers and Paw U, 1986; Pyles et al., 2000; Pyles et al., 2004; Chang et al., 2018). ACASA includes nine sunlit leaf angle classes based on a spherical leaf distribution and one shaded leaf class, for each vertical layer. The default ten vertical canopy layers therefore produce 100 different leaf classes to detail canopy structural and functional properties. ACASA has been used to accurately simulate vertical microclimatic profiles within canopies and exchanges from land surfaces in a variety of ecosystems as a stand-alone diagnostic model (Meyers and Paw U et al., 1986; Pyles et al., 2000; Pyles et al., 2004; Staudt et al., 2010; Chang et al., 2018). It has been coupled with regional scale atmospheric models to realistically represent land surface

characteristics (Pyles et al., 2003; Falk et al., 2014; Xu et al., 2014).

The ACASA-CN model used in this study is developed by coupling the ACASA model described in Chang et al. (2018), and the biogeochemical processes described in Oleson et al. (2013). The integration of biogeophysical and biogeochemical processes in ACASA-CN is similar to the coupling procedure applied in CLM4.5 (Oleson et al., 2013), except solving the biogeophysical processes with ACASA. Energy fluxes and turbulence characteristics are simulated within multiple canopy layers by ACASA, which drive the biogeochemical modules adapted from CLM4.5. Instead of applying a potential photosynthesis rate without any stress, the rate of plant photosynthesis is downregulated by nitrogen availability based on the fully prognostic CN biogeochemistry (Oleson et al., 2013). The simulated carbon cycle is then used to determine time-dependent canopy structure (growth) based on plant allometric principles (Thornton et al., 2002; Thornton and Zimmermann, 2007). Finally, the updated vegetation structure is used to provide plant morphological conditions at the next model time step to incorporate the interactions between vegetation structure and turbulence transport.

The coupling techniques described above enables ACASA-CN to utilize most of the advantages featured in both ACASA and CLM4.5 and thus in principle, ACASA-CN should be more suitable to represent terrestrial ecosystem interactions with climate and climate change. The accelerated decomposition technique proposed by Thornton and Rosenbloom (2005) is applied in ACASA-CN to reduce model spinup time for the fully prognostic carbon and nitrogen cycles.

The ACASA-CN model is driven by seven meteorological variables and carbon dioxide concentration above the canopy at half-hourly to hourly time intervals. The meteorological variables are specific humidity, precipitation, downwelling shortwave radiation, downwelling longwave radiation, air temperature, air pressure, and wind speed. In this study, these input variables were obtained from measurements taken at six AmeriFlux sites (Table 1). A static atmospheric nitrogen deposition, combining wet and dry deposition of NO_x and NH_3, is set at 0.1600056 (gN/m^2yr) as given in WRF-CLM (Wang et al., 2015). The biological nitrogen fixation is calculated as a function of net primary production, as described in CLM 4.5 (Oleson et al., 2013).

2.3. AmeriFlux network

Data from the AmeriFlux network (Baldocchi et al., 2001) were used to provide meteorological inputs for ACASA-CN, and evaluate the performance of the ACASA-CN energy, water vapor and carbon flux simulations.

We selected six AmeriFlux sites across the continental United States, to represent a range of microclimatic conditions and vegetation types (Table 1): (1) The evergreen needleleaf Blodgett Forest site (USBlo; Goldstein et al., 2000) located in California, (2) The evergreen needleleaf Duke Forest Loblolly Pine site (USDk3; Lai and Katul, 2000) located in North Carolina, (3) The deciduous broadleaf Harvard Forest site (USHa1; Moore et al., 1996) located in Massachusetts, (4) The evergreen needleleaf Howland Forest site (USHo1; Hollinger et al., 1999) located in Maine, (5) The C3 grassland Vaira Ranch site (USVar; Baldocchi et al., 2004) located in California, and (6) The evergreen needleleaf Wind River Forest (USWrc; Falk et al., 2008) located in Washington. These vegetation types cover the evergreen phenology, seasonal-deciduous phenology and stress-deciduous phenology defined in CLM4.5; therefore, they are representative for the purposes of model evaluation. More detailed descriptions for these six AmeriFlux sites can be found in Chang et al. (2018) and on the AmeriFlux website (http://ameriflux.lbl.gov/). In this study, we used eddy covariance data from 2000 to 2006 because during this period both MODIS (MODerate-resolution Imaging Spectroradiometer) Leaf Area Index (LAI) products (see section 2.4) and the AmeriFlux dataset were relatively complete. However, only the data from 2001 to 2006 were used at USVar, because much of the meteorological data required for model inputs were missing in 2000.

Quality control was applied to eddy covariance data to avoid comparing simulation results with inaccurate data (Pyles et al., 2000; Chang et al., 2018). Observations that meet the following three criteria were screened out: (1) data taken during and immediately following a precipitation event, (2) data taken when turbulence strength was weak as indicated by low friction velocity u* (0.1 m/s; Reichstein et al., 2005), and (3) the measured turbulent energy fluxes did not meet the energy budget closure criteria defined as within a 20 percent error of the available energy. Our results suggested that most of the measurements taken under weak turbulence were screened out by our energy budget closure filter, so our results were not very sensitive to the choice of u* value.

2.4. MODIS LAI product

The LAI derived from the MODIS instrument aboard the polar-orbiting Terra satellite was used to represent the time variation of canopy structures at the investigated sites. The MODIS LAI is reported to have root mean square errors ranging from 0.7 to 1.5 m^2/m^2 when compared with field measured LAI (Yang et al., 2006; Fang et al., 2012). Studies have shown that the MODIS LAI can be underestimated due to the saturation of signals in dense forests (Anav et al., 2013; Murray-Tortarolo et al., 2013). Note that although LAIs from field measurements at the AmeriFlux sites were available for a limited time period (Baldocchi et al., 2004; Thomas and Winner, 2000; Wilson et al., 2002; Sprintsin et al., 2012), they were too sparse to represent detailed continuous time evolution of canopy structure patterns over the investigated time period.

We compared the temporal variations of LAI from ACASA-CN simulations with MODIS Collection 5 LAI (MYD15A2) data during 2000 to 2006 at the six AmeriFlux sites, in addition to measured LAI reported at each site. The MYD15A2 product is retrieved based on three dimensional radiation transfer theory (Myneni et al., 2002) to produce a global 8-day composite LAI dataset with a 1-km resolution. Only LAI data that passed the quality controls of excluding cloudy, saturation, and large algorithm uncertainty conditions (Myneni et al., 2003), were used. The time evolution of the MODIS LAI from 2000 to 2006 at the six AmeriFlux sites can be found in Chang et al. (2018).

2.5. Experimental design

In order to evaluate the ACASA-CN performance and the effects of CN biogeochemistry at a site-level scale, we conducted three sets of experiments at the six AmeriFlux sites. For each site, the ecosystem type

Table 1
The AmeriFlux sites investigated in this study.

Site name	Vegetation type (IGBP)	Climate condition (Köppen)	Coordinates
Blodgett Forest (US-Blo)	Evergreen needleleaf Forest	Mediterranean (Csa)	38.8952 °N, 120.6327 °W
Duke Forest Loblolly Pine (US-Dk3)	Evergreen needleleaf Forest	Humid Subtropical (Cfa)	35.9782 °N, 79.0942 °W
Harvard Forest (US-Ha1)	Deciduous broadleaf Forest	Warm Summer Continental (Dfb)	42.5378 °N, 72.1715 °W
Howland Forest Main (US-Ho1)	Evergreen needleleaf Forest	Warm Summer Continental (Dfb)	45.2041 °N, 68.7402 °W
Vaira Ranch (US-Var)	Grasslands	Mediterranean (Csa)	38.4067 °N, 120.9507 °W
Wind River Field Station (US-Wrc)	Evergreen needleleaf Forest	Mediterranean (Csb)	45.8205 °N, 121.9519 °W

was specified by the plant functional type defined in CLM4.5 (Oleson et al., 2013), and the meteorological drivers required by ACASA-CN were provided by continuous AmeriFlux site measurements from 2000 to 2006 (2001 to 2006 for USVar).

The first set of simulations (experiment CN-ON), whose CN biogeochemistry was activated, was designed to evaluate the performance of the fully prognostic ACASA-CN model. We ran ACASA-CN initially from bare ground with CN biogeochemistry for 511 years (510 years for USVar) to have the simulated ecosystem reach its quasi-steady state under the given atmospheric nitrogen deposition (section 2.2). ACASA-CN was driven recursively by continuous meteorological measurements collected at the six AmeriFlux sites over the 7 years period 2000–2006 (6 years for USVar, 2001-2006), for the entire simulation period. The simulation results in the last 7 years (6 years for USVar) thus represent the quasi-steady state results for the climatology of these years, which were evaluated by the vegetation structure and eddy covariance measurements taken at the six AmeriFlux sites.

The second set of simulation experiments, CN-OFF, was designed to investigate the effects of omitting CN biogeochemistry on land surface simulation, by comparing with CN-ON experiments. Specifically, we ran the ACASA-CN model with carbon only biogeochemistry from 2000 to 2006 (2001 to 2006 for USVar). The vegetation structure at each site was prescribed by the quasi-steady state vegetation structure simulated by experiment CN-ON, so experiments CN-ON and CN-OFF differ only from the use of biogeochemistry.

The third set of simulations, experiment CN-OFF-RS, was designed to evaluate the performance of the quasi-steady state vegetation structure simulated by ACASA-CN. In these experiments, the ACASA-CN model was run with carbon only biogeochemistry from 2000 to 2006 (2001 to 2006 for USVar), and the vegetation structure at each site was prescribed by the remotely sensed MODIS LAI product (MYD15A2), in contrast to experiment CN-OFF.

Filling missing input data was performed to allow continuous model simulation throughout 2000 to 2006. For blocks of missing data shorter than or equal to 2 h, a linear interpolation from neighboring measurements was used to fill in data gaps. For blocks of missing data longer than 2 h, data were filled with values of the same time window averaged from the measurements taken at that week (or month, if the measurements of the entire week were missing). However, all of the simulation results driven by gap-filled data were excluded when we performed model evaluation to avoid potential biases caused by gap-filled model inputs.

The simulation results from all three sets of experiments were evaluated by measurements of the energy, water vapor and carbon fluxes at the six AmeriFlux sites. The quasi-steady state vegetation structure simulated by CN-ON was evaluated by the LAI retrievals from the MODIS MYD15A2 product and in-situ vegetation structure measurements. The impacts of CN biogeochemistry on land surface water vapor and carbon fluxes simulation was investigated by analyzing the differences between experiments CN-ON and CN-OFF. The Net Ecosystem Exchange (NEE) strengths with and without downregulation to nitrogen availability were analyzed in experiment CN-ON. The NEE with no nutrient limitations was defined as the potential NEE (pNEE), which reflects potential carbon assimilation rate and can be used to estimate the strength of nitrogen downregulation.

3. Results and discussion

3.1. Prognostic canopy structure evaluation

The time evolution of the maximum annual LAI simulated by experiment CN-ON reaches a quasi-steady state after 100–200 years of the model spinup time (Fig. 1), as suggested by Oleson et al. (2013). The periodic oscillations shown in the simulated LAI curves are artifacts caused by the 7 years (6 years for USVar) recursive cycle of input meteorological variables. The quasi-steady state LAI at each site (hereafter ACASA-LAI) was defined as the half hourly LAI simulated by ACASA-CN during the last 7 simulation years (last 6 simulation years for USVar).

The ACASA-LAI simulated at the six AmeriFlux sites was evaluated in terms of its magnitude and seasonal variability. The seasonal variability of ACASA-LAI was validated by the MODIS LAI product (hereafter MODIS-LAI), because continuous local high frequency LAI measurements at each site were not available for the study period. To unify the temporal resolutions between ACASA-LAI and MODIS-LAI, both LAI datasets were temporally smoothed and compared at the monthly scale (Fig. 2). The LAI from direct measurements reported at each site (Baldocchi et al., 2004; Thomas and Winner, 2000; Wilson et al., 2002; Sprintsin et al., 2012) were plotted to serve as a reference for the LAI magnitude (Fig. 2). During the growing season, the magnitude of ACASA-LAI agrees reasonably well with site measurements, and it is generally higher than MODIS-LAI. The amount of ACASA-LAI was greater than that of the measured LAI at USBlo and USVar, and was smaller than that at the other sites. Compared to ACASA-LAI, MODIS-LAI was smaller than the measured LAI by an even greater amount for all sites. The lower magnitude of LAI shown in MODIS-LAI during the growing season could be caused by signal saturation (Anav et al., 2013; Murray-Tortarolo et al., 2013), fine scale spatial heterogeneity, and the signal retrieval algorithm (Chang et al., 2018). During the senescent season, ACASA-LAI presents a complete leaf abscission structure (i.e., zero LAI) for ecosystems with deciduous phenology, while MODIS-LAI exhibits non-zero background LAI at USHa1 and USVar. The reason for this discrepancy is that the plant offset period simulated in ACASA-CN would be initiated by (1) sustained period of dry soil, (2) sustained period of cold temperature, or (3) less than a 6-h daytime length for ecosystems with deciduous phenology, and the plant offset period continues until the triggers of plant onset are satisfied (Oleson et al., 2013). However, plant leaves might not fall off completely during the senescent season, and background LAI could result from the presence of evergreen species at these deciduous-dominated sites, as potentially indicated by MODIS-LAI.

ACASA-LAI simulates weak seasonality for ecosystems with evergreen phenology, while MODIS-LAI shows distinct plant onset and offset periods at some of the evergreen forests, such as USDk3 and USHo1. This discrepancy could result from the exaggerated seasonal course of MODIS LAI (Heiskanen et al., 2012), and the presence of some deciduous trees or understory species at these evergreen-dominated sites. Nevertheless, it is also possible that an implementation of a stronger seasonal cycle is necessary for evergreen phenology in ACASA-CN. For ecosystems with deciduous phenology, the plant onset and offset periods align reasonably well between ACASA-LAI and MODIS-LAI. Nevertheless, we found that the soil water stress days originally defined in CLM4.5 was too weak to support plant offset at the Mediterranean grassland USVar, resulting a prolonged growing season (around 10 months). This model bias was corrected by increasing the water stress days for the leaf onset trigger, which is 8 times stronger than the parameter originally used in CLM4.5.

For evergreen forests, MODIS-LAI exhibits stronger variability and weaker magnitude as compared to ACASA-LAI (Fig. 3), similar to the monthly mean patterns shown in Fig. 2. For the deciduous forest (USHa1), the mean and variability of LAI are comparable between MODIS-LAI and ACASA-LAI, although the distribution patterns are quite different. The median of ACASA-LAI is cut off at zero, because the simulated growing season and senescent season are approximately the same duration at USHa1. On the other hand, MODIS-LAI distributes more evenly across the LAI range, because the non-zero background LAI presents over the senescent season (Fig. 2). For the C3 grassland (USVar), the simulated LAI variability is slightly greater than the remote sensing counterpart mainly due to the overestimated LAI in the growing season and underestimated LAI in senescent season (Fig. 2). The impacts of different LAI variation patterns on biogeophysical and biogeochemical simulations will be further examined in section 3.3.

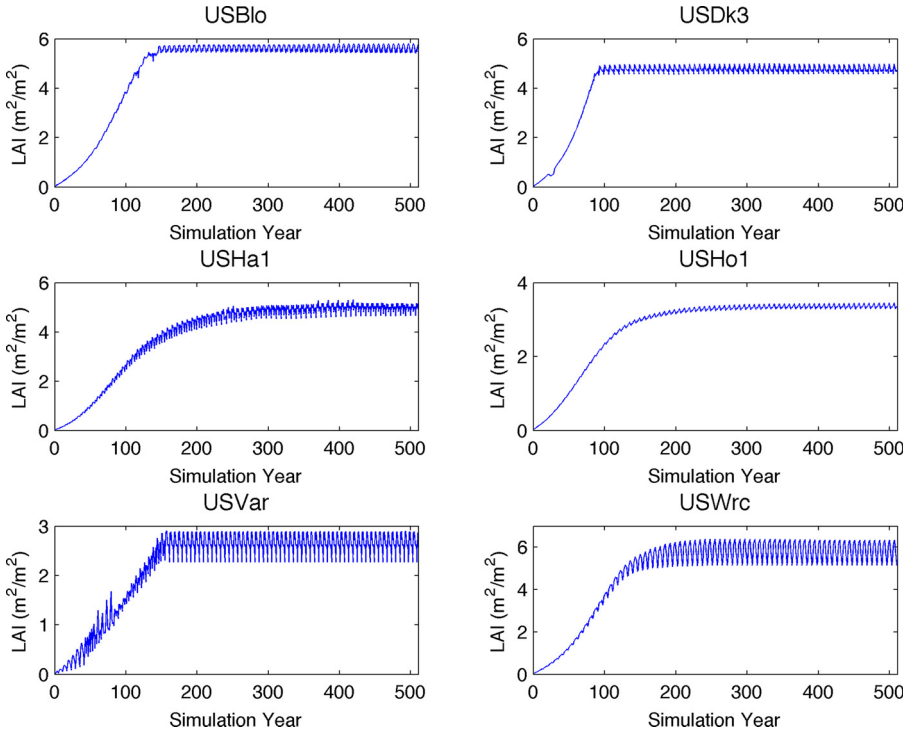

Fig. 1. Time evolution of maximum annual LAI simulated by ACASA-CN at the six AmeriFlux sites. Site names are indicated on the top of each plot and site details are given in Table 1.

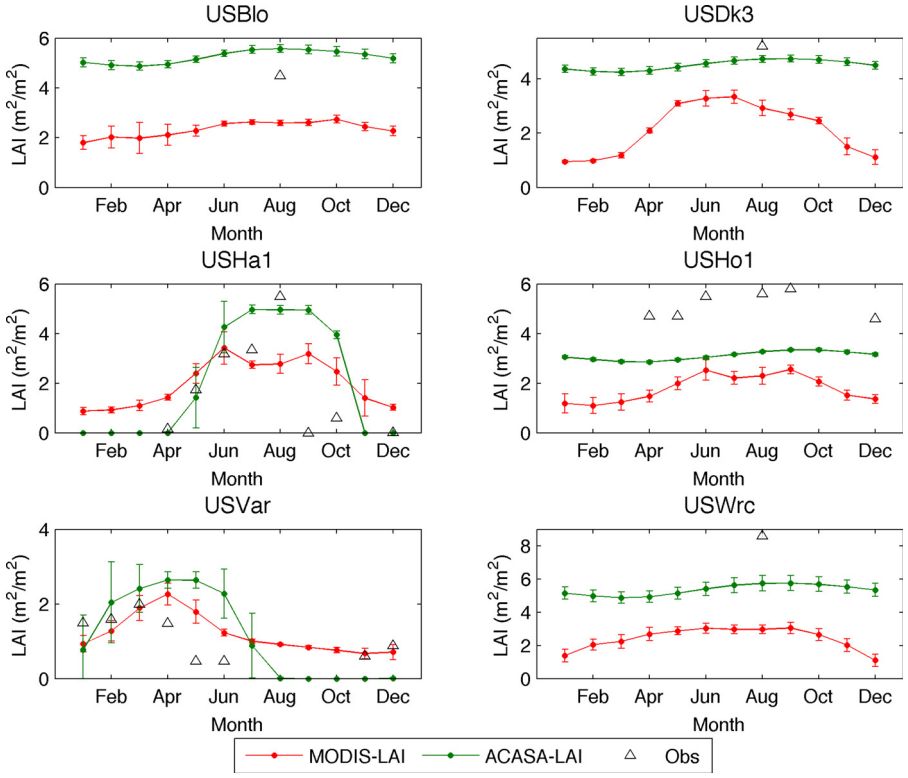

Fig. 2. The monthly mean LAI calculated from the 8-day composite LAI remotely sensed by MODIS and simulated by ACASA-CN at the six AmeriFlux sites. Error bars are the monthly LAI standard deviation during the study period. LAI site measurements at the AmeriFlux sites (Table 1) are denoted as the black triangles.

The time evolution of the canopy height simulated by ACASA-CN in experiment CN-ON reaches quasi-steady state after 100–200 years model spinup time (Fig. 4), similar to the maximum LAI pattern (Fig. 1). This is because the simulated canopy height is a function of the amount plant tissue carbon storage, set by plant allometric parameters (Oleson et al., 2013), which are related to the LAI. The simulated steady state canopy height agrees reasonably with the measured canopy heights recorded on the AmeriFlux website (http://ameriflux.lbl.gov/). However, one of the allometric parameters defined in CLM4.5, the height to the diameter at breast height ratio (taper), is too low for the ancient

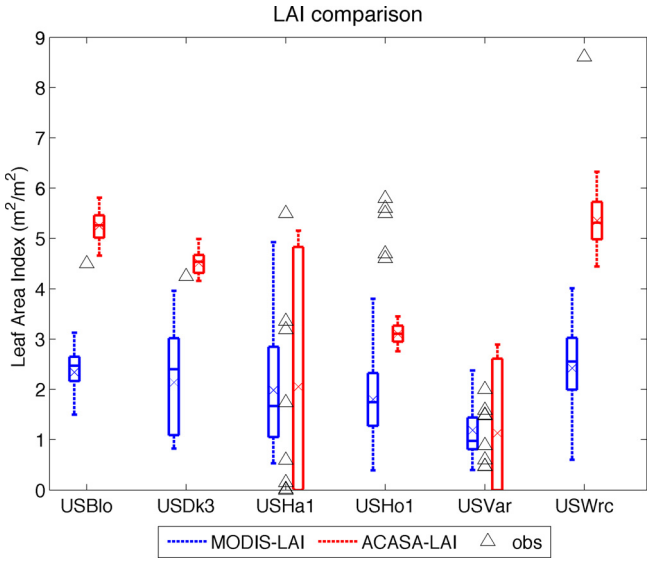

Fig. 3. Boxplots for the LAI values remotely sensed by MODIS instrument (blue) and those simulated by ACASA-CN (red) at the six AmeriFlux sites. On each box, the central mark is the median, the cross is the mean, and the lower and upper edges of the box are the 25th and 75th percentiles, respectively. The whiskers extend to the extreme values at each LAI dataset. LAI site measurements at the AmeriFlux sites (Table 1) are denoted as the black triangles (For interpretation of the references to colour in this figure legend, the reader is referred to the web version of this article).

Douglas-fir and western hemlock located at USWrc, which leads to an underestimated canopy height at steady state. Instead, we used a modified taper 4.5 times greater than the CLM4.5 default value, based on the range of in-situ measured taper values reported in the Pacific Northwest region for similar coniferous ecosystems (Eng et al., 2012; Hann et al., 1999).

Overall, the simulation results show that the prognostic canopy structure scheme used in ACASA-CN can reproduce reasonable vegetation structure such as canopy architecture and plant phenology at a site-level scale. Based on the CN biogeochemistry formulated in CLM4.5, the ACASA-CN developed here can simulate vertically resolved canopy structure profiles that adjust with microclimatic conditions at each model time step. The ACASA-CN model is thus beneficial to investigating the interactions between time varying vegetation structure, plant physiology and turbulence processes. The multiple canopy layer configuration used in ACASA-CN has advantages in resolving vertical canopy radiation energy transfer processes, which is helpful in estimating solar energy competition inside plant canopy and thus reduces model uncertainty in vegetation structure simulation.

3.2. Energy and carbon fluxes with carbon-nitrogen biogeochemistry

The performance of the biogeophysical and biogeochemical processes simulated by ACASA-CN (experiment CN-ON) was evaluated by comparing simulated and measured sensible heat, latent heat, and carbon fluxes. ACASA-CN simulates energy and carbon fluxes reasonably well, although the simulated NEE strength is underestimated under the current model configuration (Table 2). The underestimated NEE magnitude could be related to the relatively low maximum rate of carboxylation by the photosynthetic enzyme Rubisco reported in CLM4 (Bonan et al., 2012), which was used in ACASA-CN. Similar bias for NEE simulation was reported in Randerson et al. (2009).

The energy fluxes simulated in experiment CN-ON were also compared with the results from experiment CN-OFF-RS (Table 2), where ACASA-CN was driven by quality controlled MODIS-LAI with carbon only biogeochemistry. The use of the fully prognostic CN biogeochemistry in ACASA-CN is as accurate as the use of properly prescribed vegetation structure (e.g., MODIS-LAI) with carbon only biogeochemistry. These results are different from those reported in CLM4 (Lawrence et al., 2011), where the mean biogeophysical simulation is degraded with the use of CN biogeochemistry primarily because the uncertainty introduced in the prognostic vegetation structure scheme. The multiple canopy layer representation and higher order closure turbulence scheme used in ACASA-CN could be a major factor in the

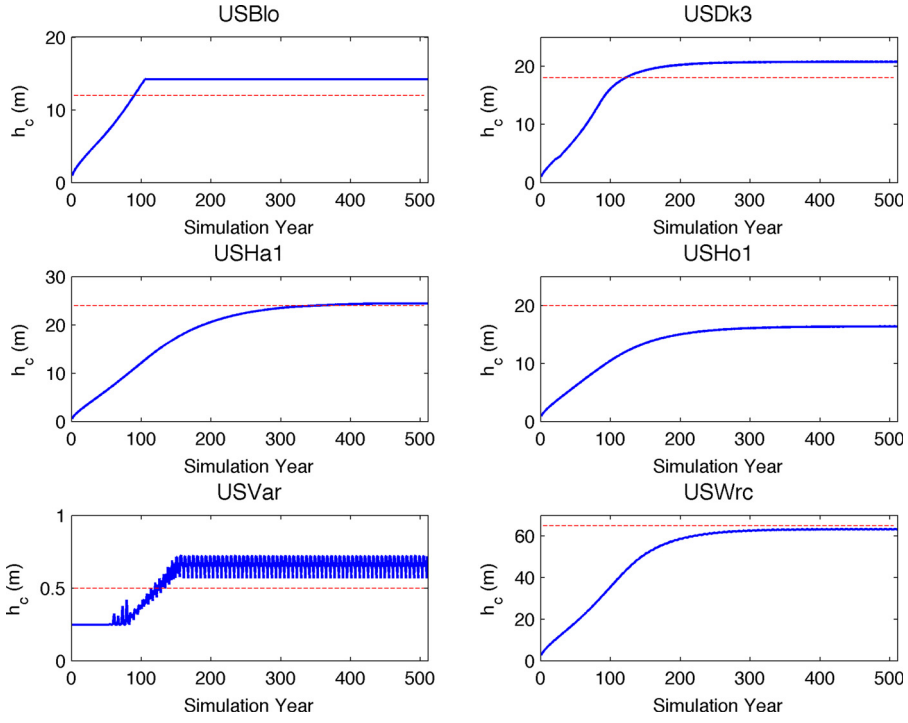

Fig. 4. Time evolution of maximum annual canopy height simulated by ACASA-CN at the six AmeriFlux sites. Red dash lines represent the measured canopy height at each site (For interpretation of the references to colour in this figure legend, the reader is referred to the web version of this article).

Table 2
Simulated sensible heat flux (H), latent heat flux (LE) and NEE for the three sets of experiments conducted in this study, compared to eddy covariance measurements at the six AmeriFlux sites detailed in Table 1. The slopes of the linear regression lines, R squared values, and root mean square errors are represented as Slope, R^2, and RMSE, respectively. Energy flux RMSE is in Wm^{-2}, and NEE RMSE is in $g\,Cm^{-2}\,s^{-1}$.

	H			LE			NEE		
	CN-ON	CN-OFF	CN-OFF-RS	CN-ON	CN-OFF	CN-OFF-RS	CN-ON	CN-OFF	CN-OFF-RS
Slope									
USBlo	1.0801	1.0197	1.0647	0.7481	0.6227	0.5187	0.6988	0.9198	0.4811
USDk3	1.2077	1.1085	1.3346	0.7350	0.6212	0.6454	0.2771	0.3475	0.2465
USHa1	0.7465	0.7519	0.8003	0.8326	0.8092	0.6952	0.3803	0.5336	0.3836
USHo1	1.0216	1. 0765	1.1090	0.8412	0.6816	0.7355	0.3301	0.4667	0.3677
USVar	0.8339	0.8481	0.9021	0.5992	0.5054	0.4547	0.5452	0.5200	0.4578
USWrc	0.8063	0.7817	0.9327	0.8670	0.5029	0.6550	0.4359	0.5587	0.3381
R^2									
USBlo	0.8684	0.7732	0.7398	0.8261	0.7479	0.6592	0.6732	0.7421	0.7015
USDk3	0.8466	0.7288	0.8509	0.8565	0.7676	0.8361	0.4683	0.4958	0.4928
USHa1	0.6796	0.6725	0.6638	0.7779	0.7766	0.7394	0.6990	0.7727	0.6908
USHo1	0.9055	0. 8484	0.9125	0.8038	0.7396	0.7881	0.6504	0.7767	0.7436
USVar	0.7532	0.7414	0.7591	0.4481	0.4323	0.5663	0.4341	0.5698	0.6388
USWrc	0.8095	0.7579	0.8297	0.4877	0.2676	0.4710	0.4002	0.4557	0.4727
RMSE									
USBlo	83.42	93.90	105.91	50.01	55.93	67.83	3.76E-05	3.42E-05	3.51E-05
USDk3	86.67	106.55	105.40	64.22	78.17	78.44	1.01E-04	8.88E-05	9.87E-05
USHa1	68.36	69.19	72.26	46.85	46.97	50.54	6.57E-05	5.21E-05	6.33E-05
USHo1	50.99	63.15	59.83	38.34	44.23	41.38	5.46E-05	4.36E-05	4.96E-05
USVar	58.57	60.85	61.42	59.56	58.09	50.93	4.25E-05	3.75E-05	3.69E-05
USWrc	78.48	88.33	84.81	73.43	70.80	64.85	6.70E-05	6.30E-05	6.34E-05

better fidelity with prognostic vegetation than with CLM4's single canopy layer paradigm, since the biogeochemical modules are mostly similar between ACASA-CN and CLM4.

ACASA-CN can reproduce reasonable energy and carbon fluxes, as shown in scatter plots between measured and simulated half-hourly energy and carbon fluxes for two selected sites, USBlo and USHa1 (Fig. 5). ACASA-CN underestimates the maximum strengths of latent heat flux and NEE, which could be caused by overestimated stomatal resistance in the simulated canopy under extreme events corresponding to the peak fluxes. Similar model bias was reported in Chang et al. (2018) when ACASA was driven by different LAI descriptions at a site-level scale. These results thus suggest that gross carbon uptake and leaf surface humidity simulated by the canopy layer processes used in ACASA may not be strong enough when the surrounding environment tends to boost the strength of ET and carbon sequestration. Further model evaluation studies are necessary to calibrate and improve the bias found in ACASA under those environmental conditions.

3.3. Energy and carbon fluxes with carbon only biogeochemistry

Energy and carbon fluxes simulated by ACASA-CN with carbon only biogeochemistry (experiments CN-OFF and CN-OFF-RS) reasonably

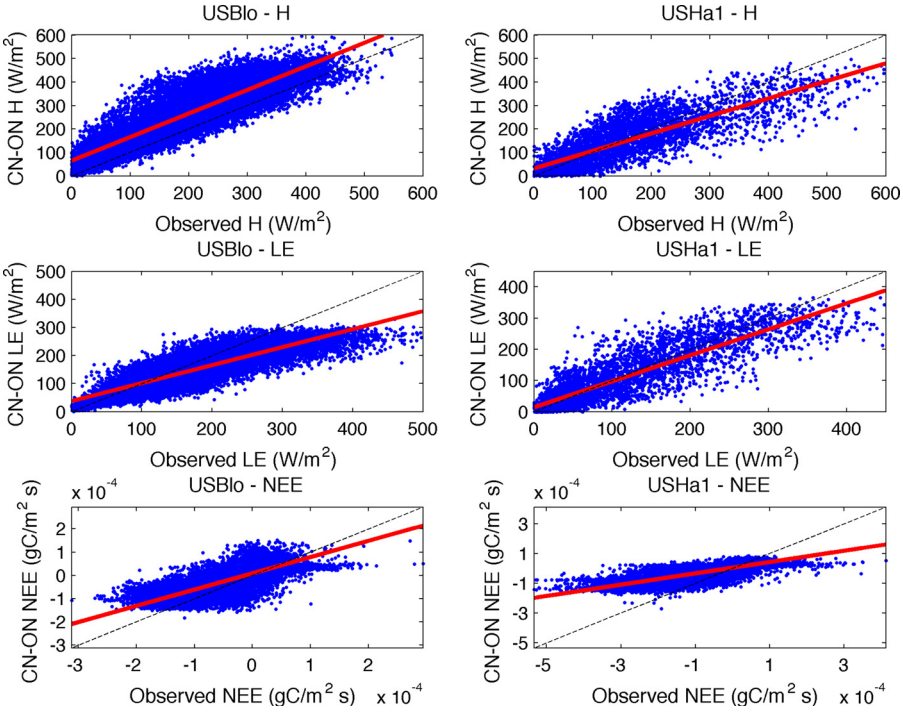

Fig. 5. Scatter plots between the observed and simulated sensible heat flux (H), latent heat flux (LE) and NEE for experiment CN-ON at USBlo and USHa1. Red lines depict the best fit linear regression equation and black dashed lines depict the one to one line. (For interpretation of the references to colour in this figure legend, the reader is referred to the web version of this article).

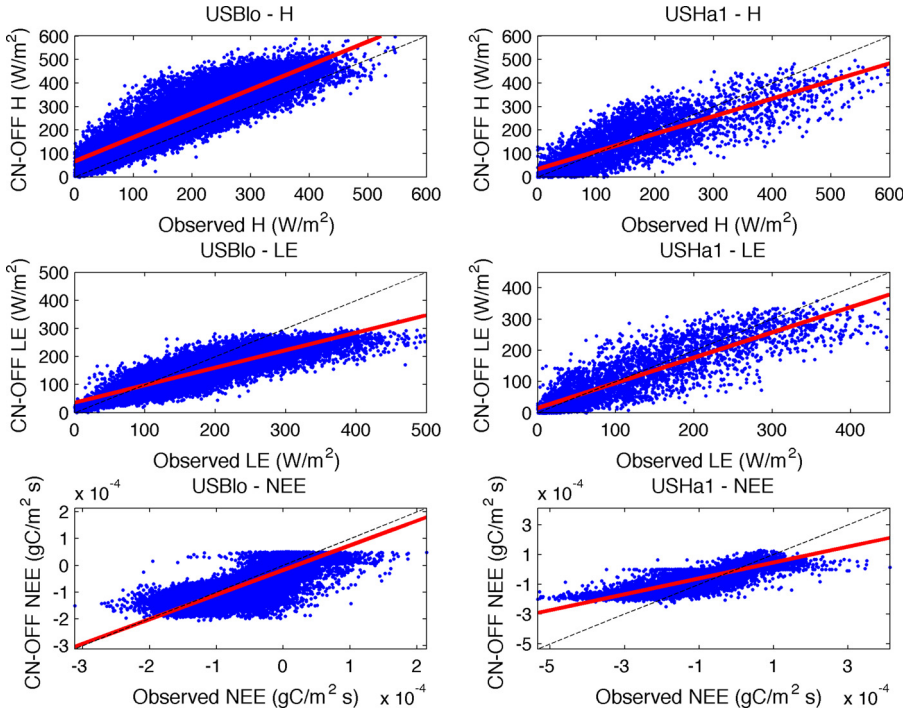

Fig. 6. The same as Fig. 5, but for experiment CN-OFF.

match the observed energy fluxes and NEE (Table 2). The results show that R squared values and root mean square errors are comparable between experiments CN-OFF and CN-OFF-RS, suggesting that ACASA-LAI is as accurate as MODIS-LAI during the study period.

Simulations and measurements agree reasonably when ACASA-CN was run with carbon-only biogeochemistry, for both sets of prescribed LAI at USBlo and USHa1 (Figs. 6 and 7). Underestimation bias for peak latent heat flux and carbon sequestration strength was found in both sets of the numerical experiments, similar to the results for experiment CN-ON (Fig. 5). Therefore, the underestimation bias under extreme events probably results from overestimated stomatal resistance inside the simulated canopy, rather than the newly introduced CN biogeochemistry or differences in the LAI used in each simulation.

Model sensitivity to different LAI descriptions (experiments CN-OFF and CN-OFF-RS), with carbon only biogeochemistry show consistent daytime behavior, as shown by results for all sites aggregated, in density scatter plots (Fig. 8). The simulated daytime latent heat flux and carbon sequestration strengths were stronger for CN-OFF than for CN-OFF-RS, probably because the amount of LAI described in ACASA-LAI is greater than those in MODIS-LAI (Fig. 2). As indicated by a steeper

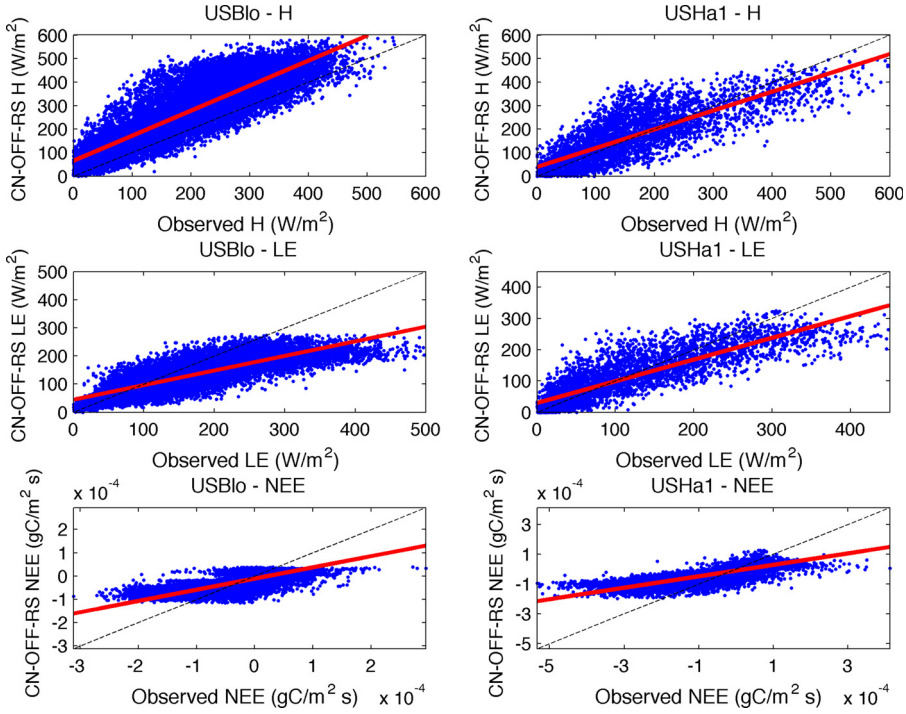

Fig. 7. The same as Fig. 5, but for experiment CN-OFF-RS.

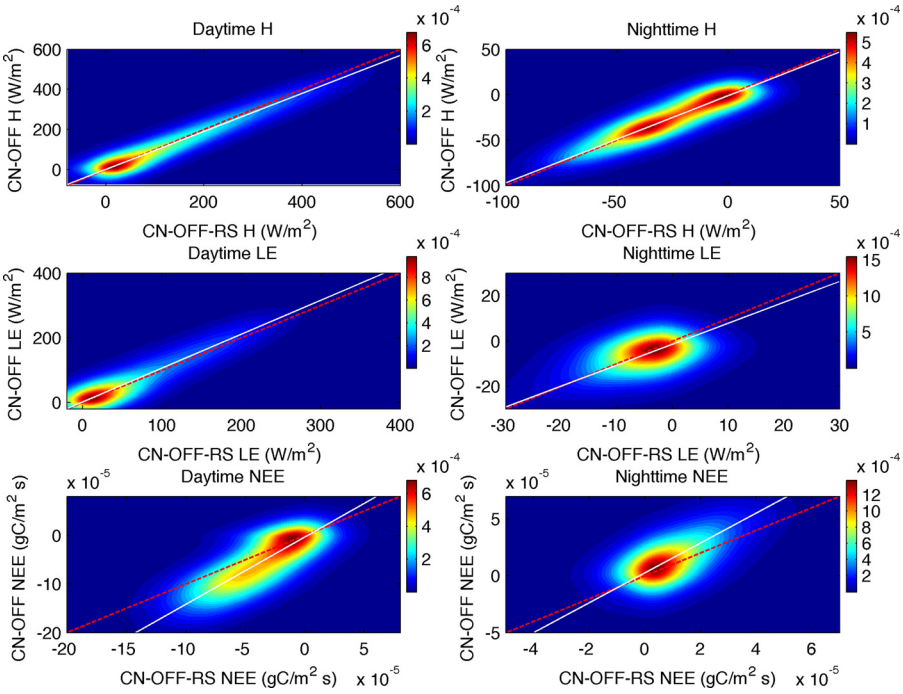

Fig. 8. Frequency of occurrence density scatter plots for the sensible heat flux (H), latent heat flux (LE) and NEE aggregated from experiments CN-OFF and CN-OFF-RS. Red dashed lines are the one to one lines, and white solid lines depict best-fit linear regression equations. (For interpretation of the references to colour in this figure legend, the reader is referred to the web version of this article).

slope shown on the density scatter plot, the simulated NEE exhibits stronger change of magnitude than the latent heat fluxes, which agrees with Chang et al. (2018) that biogeochemical processes are more sensitive to vegetation structure descriptions than the ET processes. The simulated sensible heat flux is generally weaker in experiment CN-OFF, because a larger portion of available energy is converted to latent heat flux (Fig. 8).

On the other hand, the nighttime energy budget simulations exhibit only small differences between experiments CN-OFF and CN-OFF-RS, because ecophysiological feedbacks (photosynthesis is a major feedback) become weaker without solar radiation (Fig. 8). The nighttime NEE simulated in experiment CN-OFF is generally higher than those in experiment CN-OFF-RS, because the simulated plant respiration increases with the greater amount of LAI prescribed in ACASA-LAI. The simulation results from experiments CN-OFF and CN-OFF-RS were examined using the two tailed Student's t-test, and the t-tests suggested that the differences in energy, water vapor and carbon fluxes simulations are statistically significant with p-values less than 0.05 (results not shown).

4. Model sensitivity to biogeochemistry

4.1. The effects of including the nitrogen biogeochemistry on energy and carbon fluxes

The simulated daytime NEE strength is moderately smaller with the use of CN biogeochemistry (experiment CN-ON) than carbon only biogeochemistry (experiment CN-OFF), for the six sites aggregated (Fig. 9). In contrast, simulated daytime latent heat flux is greater when including the nitrogen cycle in experiment CN-ON. Although this may seem to contradict the NEE results, they do not because daytime NEE (photosynthesis) is directly constrained by nitrogen limitations, whereas ET is not greatly affected (Oleson et al., 2013; Ghimire et al., 2016). Nighttime energy budgets are close to identical between the two biogeochemical schemes, as there is little direct control by biogeochemistry to the nighttime energy budget. The simulated NEE from the carbon only biogeochemistry is of lower magnitude than with nitrogen is included, indicating ecosystem respiration is greater when the nitrogen cycle is included, consistent with Oleson et al. (2013)'s findings.

Daytime potential NEE (pNEE), which omits photosynthetic downregulation due to nitrogen availability, aggregated over all sites, is of greater magnitude with nitrogen biogeochemistry included (Fig. 10). Because this is the opposite of the NEE comparison shown in Fig. 9, it means that nitrogen downregulation is a major control of daytime NEE. The bulk stomatal resistance calculated in the simulated canopies, however, only presents limited variation between experiments CN-ON and CN-OFF (Fig. 10), suggesting that the differences shown in water vapor and carbon fluxes simulation may not directly result from stomatal resistance. Instead, leaf temperature drops with the use of CN biogeochemistry, altering energy partitioning and water vapor pressure at the leaf surface, which contributes to shifts shown in sensible heat, latent heat and carbon fluxes. Therefore, the results show that biogeophysical processes in ACASA-CN support stronger daytime ET and carbon uptake in experiment CN-ON, but biogeochemical processes in ACASA-CN downregulate carbon uptake strength with no corresponding alterations in stomatal resistance and thus ET strength. The nocturnal pNEE simulation comparison is similar to those for NEE (Figs. 9 and 10), indicating little effect of nitrogen downregulation when photosynthesis is not involved.

The simulation results (i.e., energy, water vapor and carbon fluxes) from experiments CN-ON and CN-OFF were examined using the two tailed Student's t-test, and the t-test suggested that the differences in model outputs are statistically significant between these two experiments with p-values less than 0.05 (results not shown).

4.2. Biogeochemical effects on diurnal cycles

The mean diurnal cycles of ET simulated by ACASA-CN with and without nitrogen biogeochemistry (experiments CN-ON and CN-OFF) qualitatively match AmeriFlux observations at the six sites, when averaged over the study period (Fig. 11). The simulation results thus suggest that ET is primarily determined by the robustness of model biogeophysics, hence ACASA-CN can reasonably simulate ET with both sets of biogeochemistry. Nevertheless, we found that the magnitude of daily mean ET increases with the use of CN biogeochemistry (Table 3), consistent with the aggregated latent heat flux shown in Fig. 9. The midday ET simulated in experiment CN-ON is higher than those in

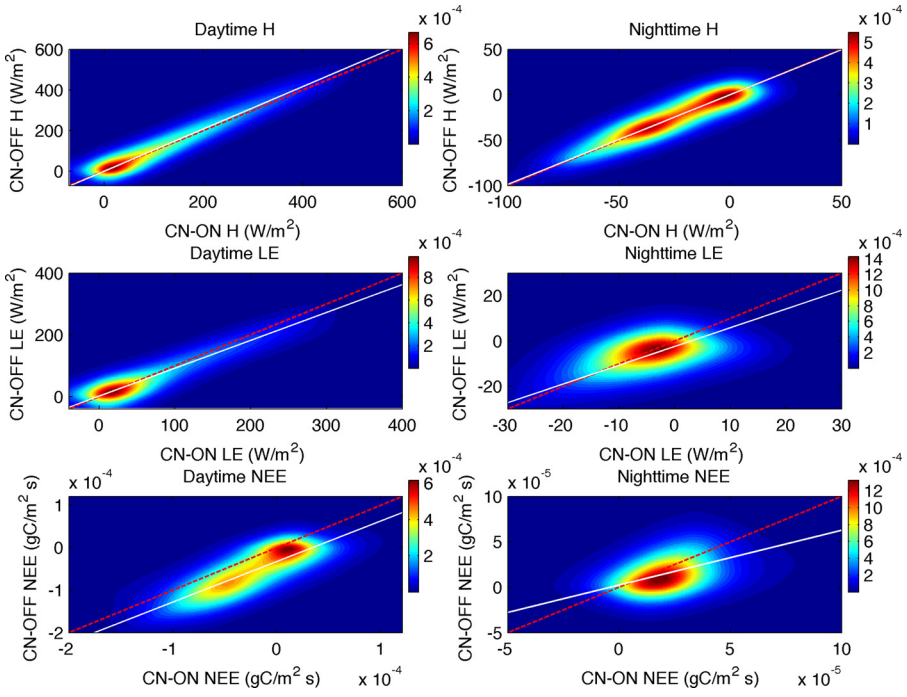

Fig. 9. Frequency of occurrence density scatter plots for the sensible heat flux (H), latent heat flux (LE) and NEE aggregated from experiments CN-ON and CN-OFF. Red dashed lines are the one to one lines, and white solid lines depict best-fit linear regression equations. (For interpretation of the references to colour in this figure legend, the reader is referred to the web version of this article).

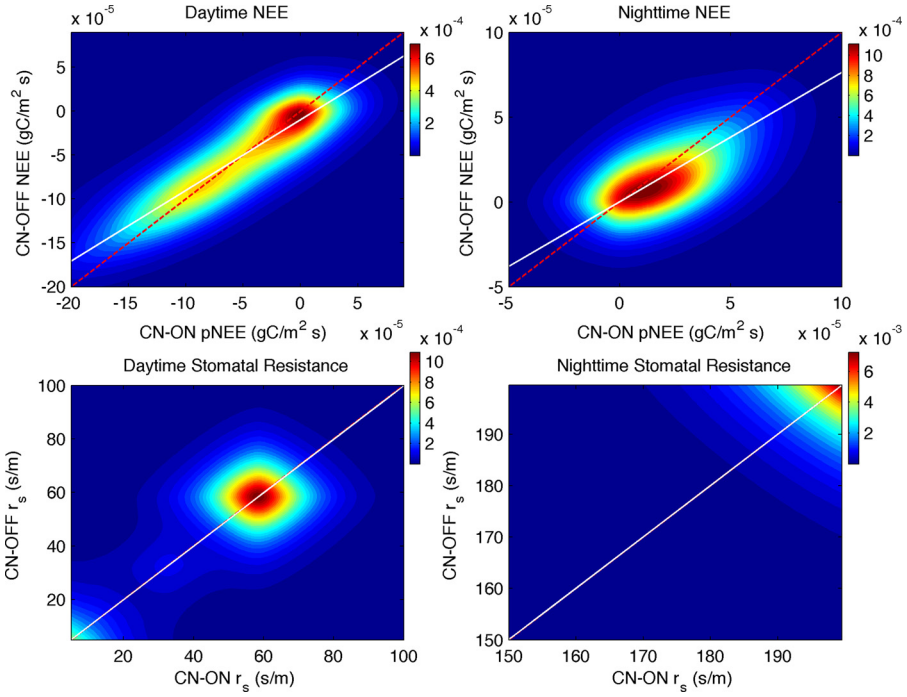

Fig. 10. Frequency of occurrence density scatter plots for the pNEE, NEE, and stomatal resistance aggregated from experiments CN-ON and CN-OFF. Red dashed lines are the one to one lines, and white solid lines depict best-fit linear regression equations. (For interpretation of the references to colour in this figure legend, the reader is referred to the web version of this article).

experiment CN-OFF, and their magnitude deviates the most at the temperate rainforest USWrc (Fig. 11).

The magnitude of simulated mean NEE diurnal cycles is weaker with the use of CN biogeochemistry (Fig. 12), consistent with the half hourly simulation results shown in Fig. 9. The diurnal transition patterns of NEE are reasonably simulated for both sets of simulations, with stronger carbon sequestration strength during midday. The mean NEE diurnal cycles simulated by ACASA-CN in experiment CN-ON do not show the unrealistic dip in daytime carbon uptake simulation reported in Ghimire et al., (2016), who used the CN biogeochemistry and single canopy layer in CLM4.5. This might suggest that ACASA-CN's multiple canopy layer representation and higher order closure turbulence scheme improve carbon flux simulation by representing more realistic canopy radiation and plant physiology processes. However, as shown in Fig. 12, the mean NEE diurnal cycles simulated in experiment CN-ON are not necessarily superior to the CN-OFF counterparts, when compared with the observed mean NEE diurnal cycles. The results suggest that the CN biogeochemistry adapted from CLM4.5 may require further calibration and adjustment to improve carbon cycle simulation under the current model configuration.

Recent studies have shown that the instantaneous downregulation applied in CLM4.5 biogeochemistry could be problematic, and models that determine photosynthesis rate by foliar nitrogen content can present more realistic biogeochemistry and improve model performance (Zaehle and Friend, 2010; Zaehle et al., 2014; Ghimire et al., 2016). Our results show that, when CN biogeochemistry is activated, the

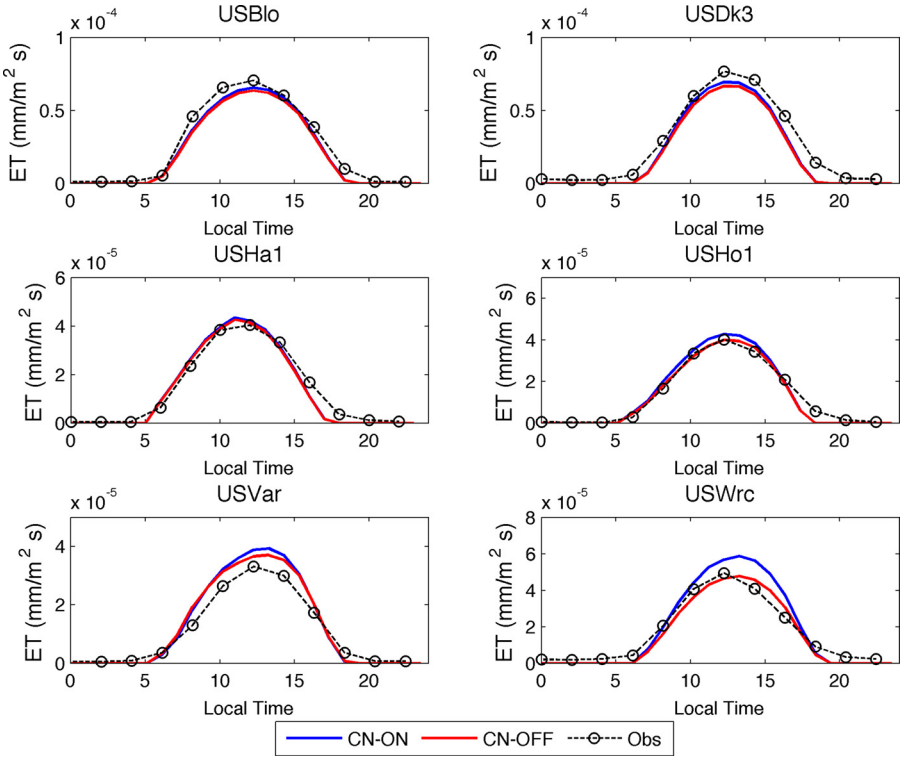

Fig. 11. The observed and simulated evapotranspiration diurnal cycles at the six AmeriFlux sites. Black dashed lines are the observed diurnal cycles averaged over the period studied, blue lines are the simulation results from experiment CN-ON, and red lines are the simulation results from experiment CN-OFF (For interpretation of the references to colour in this figure legend, the reader is referred to the web version of this article).

instantaneous downregulation is too rigorous in limiting the photosynthesis rate, resulting in an underestimation bias for NEE. This type of instantaneous downregulation takes place at the end of each model time step, and there are no signs to suggest direct effects of the downregulated actual photosynthesis relate to stomatal resistance and canopy ET (Figs. 9 and 10). Future study should aim to improve the fidelity of the instantaneous downregulation approach and the coupling between biogeophysical and biogeochemical processes.

4.3. Biogeochemical effects on the partition of evaporation and transpiration

The results from experiments CN-ON and CN-OFF show that water exchange between canopy and atmosphere is primarily through plant transpiration instead of evaporation (Fig. 13), which agrees with previous studies using isotope measurements and model simulations (Lawrence et al., 2007; Sutanto et al., 2012). The simulated transpiration at the six AmeriFlux sites is greater with the use of CN biogeochemistry (Fig. 13), which is consistent with the trend shown in the simulated ET (Fig. 11). The simulated evaporation, on the other hand, does not exhibit a similar magnitude trend at the six AmeriFlux sites, suggesting that the simulated evaporation is less sensitive to the use of biogeochemistry than the simulated transpiration examined by the ACASA-CN model.

The daily mean evaporation, transpiration and ET simulated by experiments CN-ON and CN-OFF show that plant transpiration contributes 78–88% of the total ET when ACASA-CN is run with CN biogeochemistry, and its contribution becomes slightly less (77–88%) with the use of carbon only biogeochemistry (Table 3). The ET partitioning obtained in both sets of simulations agrees with recent isotope measurements that suggest transpiration represents 80–90% of terrestrial ET (Jasechko et al., 2013). The simulated evaporation, transpiration, and ET increase 2–16%, 2-23% and 2-21%, respectively, when CN biogeochemistry is used instead of carbon only biogeochemistry (Table 3). Our results show that the response of ET to model biogeochemistry stems from the sensitivity of physiologically controlled transpiration to biogeochemical processes, while evaporation from soil and canopy surfaces is less sensitive to biogeochemical controls.

When the simulated daytime evaporation and transpiration are averaged into individual LAI windows with 0.5 m^2/m^2 increment, the results aggregated from the six sites indicate that water vapor fluxes generally increase with greater LAI regardless of the use of biogeochemistry (Fig. 14). The use of CN biogeochemistry generally enhances the daytime evaporation and transpiration averaged in each LAI window, and its effect is more prominent with higher LAI. The coherent relationship between water vapor flux and LAI exhibits in all of the

Table 3
The daily mean evaporation (E), transpiration (T) and evapotranspiration (ET) simulated from experiments CN-ON and CN-OFF at the six AmeriFlux sites. The unit for the water fluxes is mm/m^2 day.

	ET		E		T		E/ET		T/ET	
	CN-ON	CN-OFF	CN-ON	CN-OFF	CN-ON	CN-OFF	CN-ON	CN-OFF	CN-ON	CN-OFF
USBlo	1.9146	1.8524	0.2384	0.2313	1.6763	1.6210	12.45%	12.49%	87.55%	87.51%
USDk3	1.8430	1.7627	0.2748	0.2646	1.5682	1.4981	14.91%	15.01%	85.09%	84.99%
USHa1	1.1972	1.1752	0.2032	0.2000	0.9940	0.9752	16.98%	17.02%	83.02%	82.98%
USHo1	1.1910	1.1100	0.1881	0.1820	1.0029	0.9280	15.79%	16.40%	84.21%	83.60%
USVar	1.0909	1.0674	0.1394	0.1369	0.9515	0.9304	12.78%	12.83%	87.22%	87.17%
USWrc	1.6438	1.3558	0.3631	0.3143	1.2807	1.0416	22.09%	23.17%	77.91%	76.83%

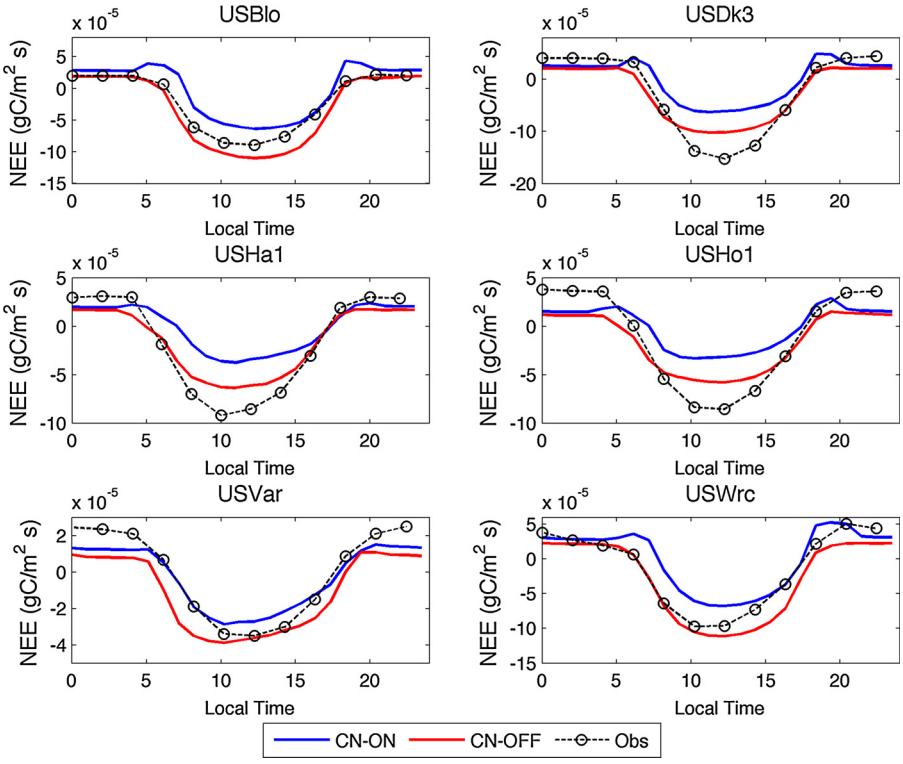

Fig. 12. The observed and simulated NEE diurnal cycles at the six AmeriFlux sites. Black dashed lines are the observed diurnal cycles averaged over the period studied, blue lines are the simulation results from experiment CN-ON, and red lines are the simulation results from experiment CN-OFF (For interpretation of the references to colour in this figure legend, the reader is referred to the web version of this article).

simulated ecosystem types, although its sensitivity slightly changes with different ecosystems. It should be noted that the apparent LAI effects are generally aligned with potential effects of seasonal and annual climatic cycles, which cannot be ruled out as other drivers of the fluxes.

Our results show that plant transpiration (T) is the main component of total ET (54–90% of total ET) throughout the LAI domain (Fig. 14), which agrees with the daily means and diurnal cycles shown above (Fig. 13). The maximum T/ET was at intermediate LAI values (~3 m^2/ m^2), with lower values at low LAI, especially for the deciduous forest (with no active leaves before leaf-out, so all ET was evaporation), regardless of whether biogeochemistry was included (Fig. 14). The contribution from transpiration starts decreasing with further increases in LAI beyond ~3 m^2/ m^2, which may arise from reduced solar radiation interception inside dense canopies because of increased self-shading, that could limit transpiration increases linked to additional amounts of

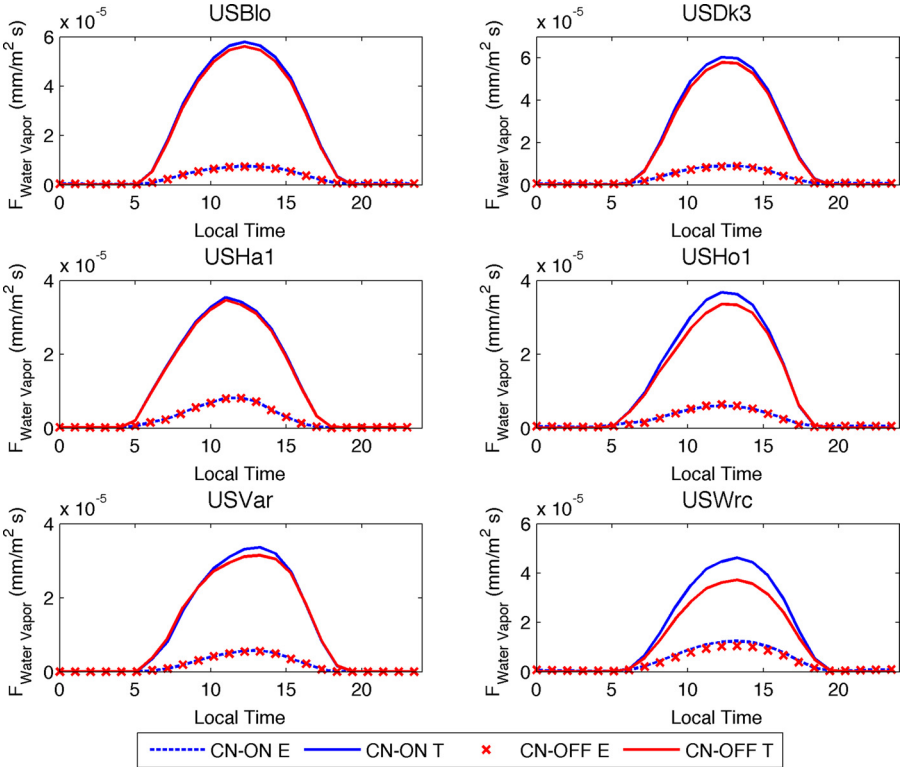

Fig. 13. The simulated evaporation (E) and transpiration (T) mean diurnal cycles at the six AmeriFlux sites during the study period. Blue dash and solid lines are the simulated evaporation and transpiration from experiment CN-ON, respectively. Red lines and crosses are the simulated evaporation and transpiration from experiment CN-OFF, respectively (For interpretation of the references to colour in this figure legend, the reader is referred to the web version of this article).

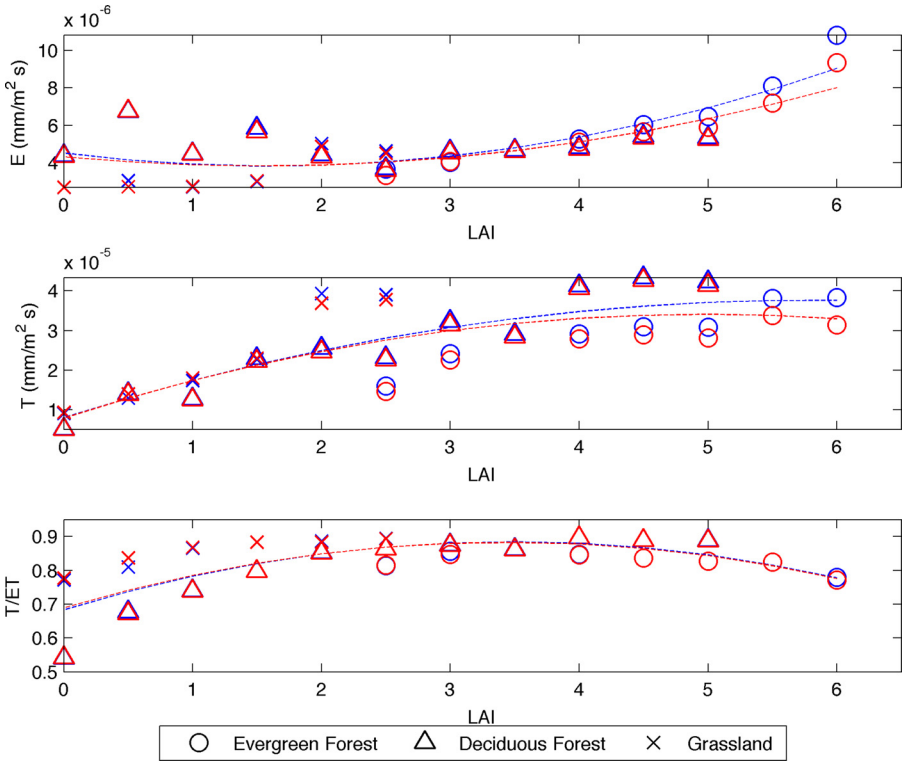

Fig. 14. Daytime evaporation (E), transpiration (T) and the ratio of transpiration to evapotranspiration (T/ET) averaged in each LAI window. Simulation results at the six AmeriFlux sites from experiments CN-ON and CN-OFF are plotted in blue and red, respectively. The results simulated at evergreen forest, deciduous forest and grassland are denoted in circle, triangle, and cross, respectively (For interpretation of the references to colour in this figure legend, the reader is referred to the web version of this article).

LAI.

Our results suggest that the partitioning of evaporation and transpiration is determined by biogeochemistry, LAI and radiation processes inside canopy. Therefore, models that do not represent the interaction of these processes with vertically resolved canopy profile may be characterized by higher uncertainty in water vapor and energy fluxes simulations.

5. Conclusions

The CN biogeochemistry and the prognostic canopy structure scheme developed in CLM4.5 were integrated into the multiple canopy layer higher order closure ACASA model. The resulting ACASA-CN model accurately portrays canopy structure (height and LAI), NEE and energy flux exchanges measured at six AmeriFlux sites, encompassing evergreen forests, deciduous forests and C3 grasslands.

Our results indicate that multiple canopy layer representation and a detailed turbulent transfer scheme are critical to ecosystem carbon uptake simulation, as an unrealistic carbon uptake pattern was found in a single canopy layer model using the same biogeochemistry (Ghimire et al., 2016). Model performance of biogeophysical energy fluxes is comparable between CN biogeochemistry with prognostic vegetation structure and carbon only biogeochemistry with observationally prescribed vegetation structure, under the ACASA-CN framework. This research shows that plant transpiration dominates ET at the examined ecosystems, representing 78% - 88% of the ET. In addition, plant transpiration is sensitive to the biogeochemical description used in models, and its magnitude generally enhanced with the use of CN biogeochemistry.

Our results indicate that the ratio of transpiration to ET exhibits a two-stage variation pattern with LAI, and it decreases in dense canopies. We also found that the instantaneous downregulation of photosynthesis rate developed in CLM4.5 may overly suppress simulated ecosystem photosynthesis. Future studies should aim to improve the model parameterization of CN biogeochemistry, and develop a more realistic functional dependency between biogeochemical and physiological processes in the simulated canopy.

Acknowledgments and Data

This research was supported through the National Science Foundation award EF1137306/MIT subaward 5710003122, the National Center of Atmospheric Research computing projectUCDV0007 to the University of California Davis, and the United States Department of Agriculture National Institute of Food and Agriculture, Hatch project CA-D-LAW-4526H and Hatch/Multistate project CA-D-LAW-7214-RR. We thank the principal investigators of the MODIS land surface products and AmeriFlux network. We thank the NASA Land Processes Distributed Active Archive Center (LP DAAC) for maintaining the MODIS land surface products, and the U.S. Department of Energy's Office of Science for funding the AmeriFlux data resources. MODIS land surface products were provided by the MODIS Land Science Team, at https://lpdaac.usgs.gov/dataset_discovery/modis/modis_products_table/myd15a2. Eddy covariance data was collected from the AmeriFlux network (http://ameriflux.lbl.gov/).

References

Anav, A., Murray-Tortarolo, G., Friedlingstein, P., Sitch, S., Piao, S., Zhu, Z., 2013. Evaluation of land surface models in reproducing satellite derived leaf area index over the high-latitude northern hemisphere. Part II: earth system models. Remote Sens. 5 (8), 3637–3661. http://dx.doi.org/10.3390/rs5083637.

Arora, V., 2002. Modeling vegetation as a dynamic component in soil-vegetation-atmosphere transfer schemes and hydrological models. Rev. Geophys. 40, 1006. http://dx.doi.org/10.1029/2001RG000103.

Baldocchi, D., et al., 2001. FluxNET: a New tool to study the temporal and spatial variability of ecosystem-scale carbon dioxide, Water vapor, and energy flux densities. Bull. Am. Meteorol. Soc. 82 (11), 2415–2434. http://dx.doi.org/10.1175/1520-0477(2001)082<2415:FANTTS>2.3.CO;2.

Baldocchi, D.D., Xu, L., Kiang, N., 2004. How plant functional-type, weather, seasonal drought, and soil physical properties alter water and energy fluxes of an oak-grass savanna and an annual grassland. Agric. For. Meteorol. 123, 13–39. http://dx.doi.org/10.1016/j.agrformet.2003.11.006.

Bonan, G.B., Lawrence, P.J., Oleson, K.W., Levis, S., Jung, M., Reichstein, M., Lawrence, D.M., Swenson, S.C., 2011. Improving canopy processes in the Community Land model version 4 (CLM4) using global flux fields empirically inferred from FLUXNET data. J. Geophys. Res. 116 (G2), G02014. http://dx.doi.org/10.1029/2010JG001593.

Bonan, G.B., Levis, S., 2010. Quantifying carbon-nitrogen feedbacks in the Community Land model (CLM4). Geophys. Res. Lett. 37 (7), L07401. http://dx.doi.org/10.1029/

2010GL042430.
Bonan, G.B., Oleson, K.W., Fisher, R.a., Lasslop, G., Reichstein, M., 2012. Reconciling leaf physiological traits and canopy flux data: use of the TRY and FLUXNET databases in the Community Land model version 4. J. Geophys. Res. Biogeosciences 117 (G2), 1–19. http://dx.doi.org/10.1029/2011JG001913.
Cox, P.M., a Betts, R., Jones, C.D., a Spall, S., Totterdell, I.J., 2000. Acceleration of global warming due to carbon-cycle feedbacks in a coupled climate model. Nature 408 (6809), 184–187. http://dx.doi.org/10.1038/35041539.
Chang, K.Y., Paw U, K.T., Chen, S.H., 2018. Canopy profile sensitivity on surface layer simulations evaluated by a multiple canopy layer higher order closure land surface model. Agric. For. Meteorol. 252, 192–207. http://dx.doi.org/10.1016/j.agrformet.2018.01.027.
Dirmeyer, P.A., Zhao, M., 2004. Flux replacement as a method to diagnose coupled land-atmosphere model feedback. J. Hydrometeorol. 5 (6), 1034–1048. http://dx.doi.org/10.1175/jhm-384.1.
Douville, H., 2003. Assessing the influence of soil moisture on seasonal climate variability with AGCMs. J. Hydrometeorol. 4 (6), 1044–1066. http://dx.doi.org/10.1175/1525-7541(2003)0041044:atiosm[2.0.co;2.
Eng, Helge, 2012. Tree height estimation in redwood/Douglas-fir stands in Mendocino County. In: Standiford, Richard B.; Weller, Theodore J.; Piirto, Douglas D.; Stuart, John D., tech. coords. Proceedings of coast redwood forests in a changing California: A symposium for scientists and managers. *Gen. Tech. Rep*. PSW-GTR-238. Albany, CA: Pacific Southwest Research Station, Forest Service, U.S. Department of Agriculture. pp. 649-654.
Falk, M., Wharton, S., Schroeder, M., Ustin, S.L., Paw U, K.T., 2008. Flux partitioning in an old-growth forest: seasonal and interannual dynamics. Tree Physiol. 28 (4), 509–520. http://dx.doi.org/10.1093/treephys/28.4.509.
Falk, M., Pyles, R.D., Ustin, S.L., Paw U, K.T., Xu, L., Whiting, M.L., Sanden, B.L., Brown, P.H., 2014. Evaluated crop evapotranspiration over a region of irrigated orchards with the improved ACASA–WRF model. J. Hydrometeorol. 15, 744–758. http://dx.doi.org/10.1175/JHM-D-12-0183.1.
Fang, H., Wei, S., Liang, S., 2012. Validation of MODIS and CYCLOPES LAI products using global field measurement data. Remote Sens. Environ. 119, 43–54. http://dx.doi.org/10.1016/j.rse.2011.12.006.
Fatichi, S., Pappas, C., Ivanov, V.Y., 2015. Modeling plant-water interactions: an ecohydrological overview from the cell to the global scale. Wiley Interdiscip. Rev. Water 3 (June), 327–368. http://dx.doi.org/10.1002/wat2.1125.
Foley, J.A., Costa, M.H., Delire, C., Ramankutty, N., Snyder, P., 2003. Green surprise? How terrestrial ecosystems could affect earth's climate. Front. Ecol. Environ. 1, 38–44. http://dx.doi.org/10.1890/1540-9295(2003)001[0038:GSHTEC]2.0.CO;2.
Friedlingstein, P., et al., 2006. Climate–Carbon cycle feedback analysis: results from the C4MIP model intercomparison. J. Clim. 19 (14), 3337–3353. http://dx.doi.org/10.1175/JCLI3800.1.
Friedlingstein, P., Meinshausen, M., Arora, V.K., Jones, C.D., Anav, A., Liddicoat, S.K., Knutti, R., 2014. Uncertainties in CMIP5 climate projections due to carbon cycle feedbacks. J. Climate 27, 511–526. http://dx.doi.org/10.1175/JCLI-D-12-00579.1.
Garratt, J.R., 1993. Sensitivity of climate simulations to land-surface and atmospheric boundary-layer treatments - a review. J. Clim. http://dx.doi.org/10.1175/1520-0442(1993)006<0419:socstl>2.0.co;2.
Ghimire, B., Riley, W.J., Koven, C.D., Mingquan Mu, A., Randerson, J.T., 2016. Representing leaf and root physiological traits in CLM improves global carbon and nitrogen cycling predictions. J. Adv. Model. Earth Syst. 8, 598–613. http://dx.doi.org/10.1002/2013MS000282. Received.
Goldstein, A.H., Hultman, N.E., Fracheboud, J.M., Bauer, M.R., Panek, J.A., Xu, M., Qi, Y., Guenther, A.B., Baugh, W., 2000. Effects of climate variability on the carbon dioxide, water, and sensible heat fluxes above a ponderosa pine plantation in the Sierra Nevada (CA). Agric. For. Meteorol. 101 (2-3), 113–129. http://dx.doi.org/10.1016/S0168-1923(99)00168-9.
Hann, M.L., Marshall, D.D., Hann, D.W., 1999. Height–diameter equations for six species in the coastal regions of the pacific northwest. For. Res. Contrib. 25.
Heiskanen, J., Rautiainen, M., Stenberg, P., Mõttus, M., Vesanto, V.-H., Korhonen, L., Majasalmi, T., 2012. Seasonal variation in MODIS LAI for a boreal forest area in Finland. Remote Sens. Environ. 126, 104–115. http://dx.doi.org/10.1016/j.rse.2012.08.001.
Hollinger, D.Y., Goltz, S.M., a Davidson, E., Lee, J.T., Tu, K., Valentine, H.T., 1999. Seasonal patterns and environmental control of carbon dioxide and water vapour exchange in an ecotonal boreal forest. Glob. Change Biol. 5 (8), 891–902. http://dx.doi.org/10.1046/j.1365-2486.1999.00281.x.
Jasechko, S., Sharp, Z.D., Gibson, J.J., Birks, S.J., Yi, Y., Fawcett, P.J., 2013. Terrestrial water fluxes dominated by transpiration. Nature 496 (7445), 347–350. http://dx.doi.org/10.1038/nature11983.
Lai, C.T., Katul, G., 2000. The dynamic role of root-water uptake in coupling potential to actual transpiration. Adv. Water Resour. 23 (4), 427–439. http://dx.doi.org/10.1016/S0309-1708(99)00023-8.
Lawrence, D.M., Thornton, P.E., Oleson, K.W., Bonan, G.B., 2007. The partitioning of evapotranspiration into transpiration, soil evaporation, and canopy evaporation in a GCM: impacts on land–atmosphere interaction. J. Hydrometeorol. 8 (4), 862–880. http://dx.doi.org/10.1175/JHM596.1.
Lawrence, D.M., Oleson, K.W., Flanner, M.G., Thornton, P.E., Swenson, S.C., Lawrence, P.J., Zeng, X., Yang, Z.-L., Levis, S., Samuel, K., Sakaguchi, G.B., Bonan, Slater, A.G., 2011. Parameterization improvements and functional and structural advances in version 4 of the Community Land model. J. Adv. Model. Earth Syst. 3 (3), 1–27. http://dx.doi.org/10.1029/2011MS000045.
Levis, S., 2010. Modeling vegetation and land use in models of the Earth System. WIREs Clim Change 1, 840–856. http://dx.doi.org/10.1002/wcc.83.
Matthews, H.D., Eby, M., Ewen, T., Friedlingstein, P., Hawkins, B.J., 2007. What determines the magnitude of carbon cycle-climate feedbacks? Glob. Biogeochem. Cycles 21 (2), 1–12. http://dx.doi.org/10.1029/2006GB002733.
Meyers, T., Paw U, K.T., 1986. Testing of a higher-order closure model for modeling airflow within and above plant canopies. Boundary Layer Meteorol. 37 (3), 297–311. http://dx.doi.org/10.1007/BF00122991.
Meyers, T.P., Paw U, K.T., 1987. TESTING OF a higher-order CLOSURE MODEL FOR MODELING AIRFLOW AND ABOVE PLANT CANOPIES. Boundary Layer Meteorol. 37, 297–311.
Moore, K.E., Fitzjarrald, D.R., Sakai, R.K., Goulden, M.L., Munger, J.W., Wofsy, S.C., 1996. Seasonal variation in radiative and turbulent Exchange at a deciduous Forest in Central Massachusetts. J. Appl. Meterol. 35, 122–134. http://dx.doi.org/10.1175/1520-0450(1996)035<0122:SVIRAT>2.0.CO;2.
Murray-Tortarolo, G., et al., 2013. Evaluation of Land surface models in reproducing satellite-derived LAI over the high-latitude Northern Hemisphere. Part i: uncoupled DGVMs. Remote Sens. 5 (10), 4819–4838. http://dx.doi.org/10.3390/rs5104819.
Myneni, R.B., et al., 2002. Global products of vegetation leaf area and fraction absorbed PAR from year one of MODIS data. Remote Sens. Environ. 83 (1–2), 214–231. http://dx.doi.org/10.1016/S0034-4257(02)00074-3.
Myneni, R., Knyazikhin, Y., Glassy, J., Votava, P., Shabanov, N., 2003. User' s Guide FPAR, LAI (ESDT: MOD15A2) 8-day composite NASA MODIS Land algorithm, FPAR. LAI User's Guid. 1–17.
Oleson, K.W., et al., 2013. Technical Description of Version 4.5 of the Community Land Model (CLM) Coordinating, NCAR/TN-503+STR NCAR Tech. Note (July). .
Pielke, R.a., et al., 2011. Land use/land cover changes and climate: modeling analysis and observational evidence. Wiley Interdiscip. Rev. Clim. Change 2 (6), 828–850. http://dx.doi.org/10.1002/wcc.144.
Pyles, R.D., Weare, B.C., Paw U, K.T., 2000. The UCD advanced canopy-atmosphere-soil algorithm: comparisons with observations from different climate and vegetation regimes. Q. J. R. Meteorol. Soc. 126 (569), 2951–2980. http://dx.doi.org/10.1002/qj.49712656917.
Pyles, R.D., Weare, B.C., Paw U, K.T., Gustafson, W., July 2003. Coupling between the University of California, Davis, Advanced canopy–atmosphere–soil algorithm (ACASA) and MM5: preliminary results for July 1998 for Western North America. J. Appl. Meteorol. 42 (5), 557–569. http://dx.doi.org/10.1175/1520-0450(2003)042<0557:CBTUOC>2.0.CO;2.
Pyles, R., Paw U, K.T., Falk, M., 2004. Directional wind shear within an old-growth temperate rainforest: observations and model results. Agric. For. Meteorol. 125, 19–31. http://dx.doi.org/10.1016/j.agrformet.2004.03.007.
Randerson, J.T., et al., 2009. Systematic assessment of terrestrial biogeochemistry in coupled climate-carbon models. Glob. Change Biol. 15 (10), 2462–2484. http://dx.doi.org/10.1111/j.1365-2486.2009.01912.x.
Reichstein, M., Falge, E., Baldocchi, D., Papale, D., Aubinet, M., Berbigier, P., Bernhofer, C., Buchmann, N., Gilmanov, T., Granier, A., Grunwald, T., Havrankova, K., Ilvesniemi, H., Janous, D., Knohl, A., Laurila, T., Lohila, A., Loustau, D., Matteucci, G., Meyers, T., Miglietta, F., Ourcival, J.M., Pumpanen, J., Rambal, S., Rotenberg, E., Sanz, M., Tenhunen, J., Seufert, G., Vaccari, F., Vesala, T., Yakir, D., Valentini, R., 2005. On the separation of net ecosystem exchange into assimilation and ecosystem respiration: review and improved algorithm. Glob. Change Biol. 11 (9), 1424–1439. http://dx.doi.org/10.1111/j.1365-2486.2005.001002.x.
Sellers, P.J., Dickinson, R.E., Randall, D.A., Betts, A.K., Hall, F.G., Berry, J.A., Collatz, G.J., Denning, A.S., Mooney, H.A., Nobre, C.A., Sato, N., Field, C.B., Henderson-Sellers, A., 1997. Modeling the exchanges of energy, Water, and carbon between continents and the atmosphere. Science 275 (5299), 502–509. http://dx.doi.org/10.1126/science.275.5299.502.
Sokolov, A.P., Kicklighter, D.W., Melillo, J.M., Felzer, B.S., Schlosser, C.A., Cronin, T.W., 2008. Consequences of considering carbon-nitrogen interactions on the feedbacks between climate and the terrestrial carbon cycle. J. Clim. 21 (15), 3776–3796. http://dx.doi.org/10.1175/2008JCLI2038.1.
Sprintsin, M., Chen, J.M., Desai, A., Gough, C.M., 2012. Evaluation of leaf-to-canopy upscaling methodologies against carbon flux data in North America. J. Geophys. Res. Biogeosci. 117 (1), 1–17. http://dx.doi.org/10.1029/2010JG001407.
Staudt, K., Falge, E., Pyles, R.D., Paw, U.K.T., Foken, T., 2010. Sensitivity and predictive uncertainty of the ACASA model at a spruce forest site. Biogeosciences 7 (11), 3685–3705. http://dx.doi.org/10.5194/bg-7-3685-2010.
Sun, Y., Gu, L., Dickinson, R.E., 2012. A numerical issue in calculating the coupled carbon and water fluxes in a climate model. J. Geophys. Res. Atmos. 117 (22), 1–16. http://dx.doi.org/10.1029/2012JD018059.
Sutanto, S.J., Wenninger, J., Coenders-Gerrits, A.M.J., Uhlenbrook, S., 2012. Partitioning of evaporation into transpiration, soil evaporation and interception: a comparison between isotope measurements and A HYDRUS-1D model. Hydrol. Earth Syst. Sci. 16 (8), 2605–2616. http://dx.doi.org/10.5194/hess-16-2605-2012.
Thomas, S.C., Winner, W.E., 2000. Leaf area index of an old-growth Douglas-fir forest estimated from direct structural measurements in the canopy. Can. J. For. Res. 30 (12), 1922–1930. http://dx.doi.org/10.1139/x00-121.
Thornton, P.E., Doney, S.C., Lindsay, K., Moore, J.K., Mahowald, N., Randerson, J.T., Fung, I., Lamarque, J.-F., Feddema, J.J., Lee, Y.-H., 2009. Carbon-nitrogen interactions regulate climate-carbon cycle feedbacks: results from an atmosphere-ocean general circulation model. Biogeosciences 6 (2), 3303–3354. http://dx.doi.org/10.5194/bgd-6-3303-2009.
Thornton, P.E., Lamarque, J.F., Rosenbloom, Na., Mahowald, N.M., 2007. Influence of carbon-nitrogen cycle coupling on land model response to CO2 fertilization and climate variability. Global Biogeochem. Cycles 21 (4), 1–15. http://dx.doi.org/10.1029/2006GB002868.
Thornton, P.E., et al., 2002. Modeling and measuring the effects of disturbance history and climate on carbon and water budgets in evergreen needleleaf forests. Agric. For. Meteorol. 113 (1–4), 185–222. http://dx.doi.org/10.1016/S0168-1923(02)00108-9.

Thornton, P.E., Rosenbloom, N.A., 2005. Ecosystem model spin-up: estimating steady state conditions in a coupled terrestrial carbon and nitrogen cycle model. Ecol. Model. 189 (1–2), 25–48. http://dx.doi.org/10.1016/j.ecolmodel.2005.04.008.

Thornton, P.E., Zimmermann, N.E., 2007. An improved canopy integration Scheme for a Land surface model with prognostic canopy structure. J. Clim. 20 (15), 3902–3923. http://dx.doi.org/10.1175/JCLI4222.1.

Wang, W., et al., 2015. ARW Version 3 Modeling system User's Guide. http://dx.doi.org/10.1525/jps.2007.37.1.204.

Weiss, M., et al., 2014. Contribution of dynamic vegetation phenology to decadal climate predictability. J. Clim. 27, 8563–8577. http://dx.doi.org/10.1175/JCLI-D-13-00684.1.

Weiss, M., van den Hurk, B., Haarsma, R., Hazeleger, W., 2012. Impact of vegetation variability on potential predictability and skill of EC-Earth simulations. Clim. Dyn. 39, 2733–2746. http://dx.doi.org/10.1007/s00382-012-1572-0.

Wilson, K.B., et al., 2002. Energy partitioning between latent and sensible heat flux during the warm season at FLUXNET sites. Water Resour. Res. 38 (12), 1–11. http://dx.doi.org/10.1029/2001WR000989.

Xu, L., Pyles, R.D., Paw U, K.T., Chen, S.H., Monier, E., 2014. Coupling the high complexity land surface model ACASA to the mesoscale model WRF. Geosci. Model. Dev. Discuss. 7 (3), 2829–2875. http://dx.doi.org/10.5194/gmdd-7-2829-2014.

Yang, W., et al., 2006. MODIS leaf Area index products: from validation to algorithm improvement. IEEE Trans. Geosci. Remote Sens. 44 (7), 1885–1898. http://dx.doi.org/10.1109/TGRS.2006.871215.

Zaehle, S., Friedlingstein, P., Friend, A.D., 2010a. Terrestrial nitrogen feedbacks may accelerate future climate change. Geophys. Res. Lett. 37 (1), 1–5. http://dx.doi.org/10.1029/2009GL041345.

Zaehle, S., Friend, A.D., 2010. Carbon and nitrogen cycle dynamics in the O-CN land surface model: 1. Model description, site-scale evaluation, and sensitivity to parameter estimates. Glob. Biogeochem. Cycles 24 (1), 1–13. http://dx.doi.org/10.1029/2009GB003521.

Zaehle, S., Friend, a.D., Friedlingstein, P., Dentener, F., Peylin, P., Schulz, M., 2010b. Carbon and nitrogen cycle dynamics in the O-CN land surface model: 2. Role of the nitrogen cycle in the historical terrestrial carbon balance. Glob. Biogeochem. Cycles 24 (1), 1–14. http://dx.doi.org/10.1029/2009GB003522.

Zaehle, S., et al., 2014. Evaluation of 11 terrestrial carbon – nitrogen cycle models against observations from two temperate free-air CO 2 enrichment studies S o. New. Phytol. 202 (3), 803–822. http://dx.doi.org/10.1111/nph.12697.